AFRL-RH-WP-TR-2011-0023

Static and Dynamic Human Shape Modeling – Concept Formation and Technology Development

Zhiqing Cheng

Infoscitex Corporation

Julia Parakkat
Melody Darby
Kathleen Robinette

Vulnerability Analysis Branch
Biosciences and Performance Division

FEBRUARY 2011
Final Report

AIR FORCE RESEARCH LABORATORY
711TH HUMAN PERFORMANCE WING
HUMAN EFFECTIVENESS DIRECTORATE
WRIGHT-PATTERSON AIR FORCE BASE, OH 45433
AIR FORCE MATERIEL COMMAND
UNITED STATES AIR FORCE

NOTICE AND SIGNATURE PAGE

Using Government drawings, specifications, or other data included in this document for any purpose other than Government procurement does not in any way obligate the U.S. Government. The fact that the Government formulated or supplied the drawings, specifications, or other data does not license the holder or any other person or corporation; or convey any rights or permission to manufacture, use, or sell any patented invention that may relate to them.

This report was cleared for public release by the 88th Air Base Wing Public Affairs Office and is available to the general public, including foreign nationals. Copies may be obtained from the Defense Technical Information Center (DTIC) (http://www.dtic.mil).

AFRL-RH-WP-TR-2011-0023 HAS BEEN REVIEWED AND IS APPROVED FOR PUBLICATION IN ACCORDANCE WITH ASSIGNED DISTRIBUTION STATEMENT.

Julia Parakkat

Julia Parakkat, Work Unit Manager
Vulnerability Analysis Branch

F. Wesley Baumgardner

F. Wesley Baumgardner, Ph.D.
Biosciences and Performance Division
Human Effectiveness Directorate
711th Human Performance Wing
Air Force Research Laboratory

This report is published in the interest of scientific and technical information exchange, and its publication does not constitute the Government's approval or disapproval of its ideas or findings.

REPORT DOCUMENTATION PAGE

Form Approved
OMB No. 0704-0188

1. REPORT DATE *(DD-MM-YYYY)*	2. REPORT TYPE	3. DATES COVERED *(From - To)*
02-28-2011	Final	January 2009 – February 2011

4. TITLE AND SUBTITLE
Static and Dynamic Human Shape Modeling – Concept Formation and Technology Development

5a. CONTRACT NUMBER
IN-HOUSE

5b. GRANT NUMBER

5c. PROGRAM ELEMENT NUMBER
62202F

6. AUTHOR(S)
Zhiqing Cheng, Julia Parakkat, Melody Darby, Kathleen Robinette

5d. PROJECT NUMBER
7184

5e. TASK NUMBER
02

5f. WORK UNIT NUMBER
71840226

7. PERFORMING ORGANIZATION NAME(S) AND ADDRESS(ES)

Vulnerability Analysis Branch
Biosciences and Performance Division
Air Force Research Laboratory

8. PERFORMING ORGANIZATION REPORT NUMBER

9. SPONSORING / MONITORING AGENCY NAME(S) AND ADDRESS(ES)
Air Force Materiel Command
Air Force Research Laboratory
711th Human Performance Wing
Human Effectiveness Directorate
Biosciences and Performance Division
Vulnerability Analysis Branch
Wright-Patterson AFB OH 45433-7947

10. SPONSOR/MONITOR'S ACRONYM(S)
711 HPW/RHPA

11. SPONSOR/MONITOR'S REPORT NUMBER(S)
AFRL-RH-WP-TR-2011-0023

12. DISTRIBUTION / AVAILABILITY STATEMENT

Distribution A: Approved for public release, distribution is unlimited

13. SUPPLEMENTARY NOTES

88ABW/PA cleared on 31 Mar 11, 88ABW-2011-1953

14. ABSTRACT
Extensive investigations were performed in this project on human shape modeling. The problem was addressed from the perspectives of static shape modeling and morphing, human shape modeling in various poses, dynamic modeling, and human activity replication/ animation. The major problems involved in each topic were identified, and the methods and techniques were developed or formulated for them. Some of these methods or algorithms were implemented, and the results were presented and discussed. Conclusions were drawn from research results and findings, the issues remaining were described, and the future work was discussed.

15. SUBJECT TERMS
Static Human Shape Modeling; Pose Change Modeling; Dynamic 3-D Human Shape Modeling, Human Activity Replication/Animation

16. SECURITY CLASSIFICATION OF:			17. LIMITATION OF ABSTRACT	18. NUMBER OF PAGES	19a. NAME OF RESPONSIBLE PERSON
a. REPORT	b. ABSTRACT	c. THIS PAGE			Julia Parakkat
U	U	U	SAR	36	19b. TELEPHONE NUMBER *(include area code)* NA

Standard Form 298 (Rev. 8-98)
Prescribed by ANSI Std. 239.18

THIS PAGE IS INTENTIONAL LEFT BLANK

TABLE OF CONTENTS

LIST OF FIGURES

SUMMARY

This report details the research performed on human shape modeling. The topics covered include static shape modeling and morphing, human shape modeling in various poses, dynamic modeling, and human activity replication/animation. The report provides a detailed description of the challenges of each topic, the methods and algorithms developed for each topic, the implementation of the methods and algorithms developed, and some computational results. The contents of the report are arranged as follows: 1. Introduction; 2. Static Shape Modeling and Morphing; 3. Shape Modeling in Various Poses; 4. Dynamic Modeling; 5. Human Activity Replication and Animation; 6. Concluding Remarks; and 7. References.

THIS PAGE IS INTENTIONAL LEFT BLANK

1.0 INTRODUCTION

Human modeling and simulation has vast applications in various areas, such as immersive and interactive virtual reality, human-machine interface and work station, game and entertainment, human identification, and human-borne threat detection. However, creating a realistic, morphable, animatable, and highly bio-fidelic human shape model is a major challenge for anthropometry and computer graphics.

Human shape modeling can be classified as either static or dynamic. Static shape modeling creates a model to describe human shape at a particular pose, usually a standing pose. The major issues involved in static shape modeling include shape description, registration, hole filling, shape variation characterization, and shape reconstruction. Dynamic shape modeling addresses shape variations due to pose changes or due to gross body motion. While pose identification, skeleton modeling, and shape deformation are the major issues involved with pose modeling, motion tracking, shape extraction, shape reconstruction, animation, and inverse kinematics are the main issues to consider for the shape modeling of humans in motion.

A static three dimensional (3-D) human shape model provides anthropometric information. A dynamic 3-D human shape model contains information on shape, pose, and gait. Constructed from 2-D video imagery or 3-D sensor data, such a model can potentially be used to depict a human's activity and behavior, to predict his intention, to uncover any disguises, and to uncover hidden objects. Therefore, human shape modeling technology can be used for suspect identification and human-borne threat detection, in addition to its traditional applications, such as ergonomic design of human spaces and workstations, creating vivid and realistic figures and action animations, and virtual design and fitting of personalized clothing.

As human modeling and simulation play a critical role in human identification and human-borne threat detection, a 6.2 program entitled, "Human Measurement Modeling," was established in the Air Force Research Laboratory for research on human shape modeling. Under the support of this program, extensive investigations were performed on static shape modeling and morphing, shape modeling in various poses (pose modeling), dynamic modeling, and human activity replication and animation. In a preceding report [1], a literature review was presented on recent developments in human shape modeling, in particular, static shape modeling based on range scan data and dynamic shape modeling from video imagery. This report describes the investigations on the methodology development, concept formation, solution formulation, and algorithm development and implementation.

2.0 STATIC SHAPE MODELING AND MORPHING

The 3-D human static shape modeling in this project is based on the 3-D laser scan data from the CAESAR (Civilian American and European Surface Anthropometry Resource) database (http://store.sae.org/caesar). For the representation of a human body shape, polygons/vertices are usually used as the basic graphic entities. Approximately 20,000 ~ 500,000 vertices are required to describe a full body shape, depending upon surface resolution. This method of surface representation incurs a large computational cost and cannot ensure point-to-point correspondence among the scans of different subjects. Instead, contour lines were proposed as the basic entities

for the shape modeling in this project. The entire procedure for static shape modeling consists of several steps: (1) joint center calculation; (2) skeleton model building; (3) segmentation; (4) slicing; (5) discretizing; (6) hole filling; (7) parameterization and shape description; (8) surface registration; (9) shape variation characterization using Principle Component Analysis (PCA); (10) feature extraction with control parameters; (11) shape reconstruction/morphing; and (12) part blending. The details of each step are described below.

2.1 Joint Center Calculation

The human body is treated as a multi-segment system where segments are connected to each other by joints. The joint centers are defined by respective landmarks, which in turn, are either measured or calculated in the CAESAR database. According to [2], major joint centers are defined by landmarks as follows:

Ankles, right and left: use midpoint between Lateral Malleolus and Sphyrion.

Knees, right and left: use midpoint between Lateral and Medial Femoral Epicondyles.

Hips, right and left: 1) start at midpoint between Anterior Superior Iliac Spine and Symphysion;

2) translate in the posterior direction to the plane of the Trochanterions;

3) translate 15 mm down.

Pelvic Joint: 1) start at Posterior Superior Iliac Midspine coordinates;

2) translate 51 mm in the anterior direction.

Abdomen Joint: 1) start at 10^{th} Rib Midspine coordinates;

2) translate 51 mm in the anterior direction.

Thorax Joint: 1) start at Cervicale coordinates;

2) translate 51 mm in the anterior direction;

3) translate 25 mm down.

Head/Neck Joint: use midpoint between right and left Tragions.

Shoulder, right and left: 1) start at Acromion coordinates;

2) translate 38 mm in the medial direction;

3) translate 38 mm down.

Elbow, right and left: use midpoint between Medial and Lateral Humeral Epicondyles

Wrist, right and left: use midpoint between Radial and Ulnar Styloid Processes

According to the 3-D landmark list for standing posture used in the CAESAR database [3], a Matlab code was developed to calculate the joints centers. **Figure 1** illustrates an example of the joint centers derived from landmarks.

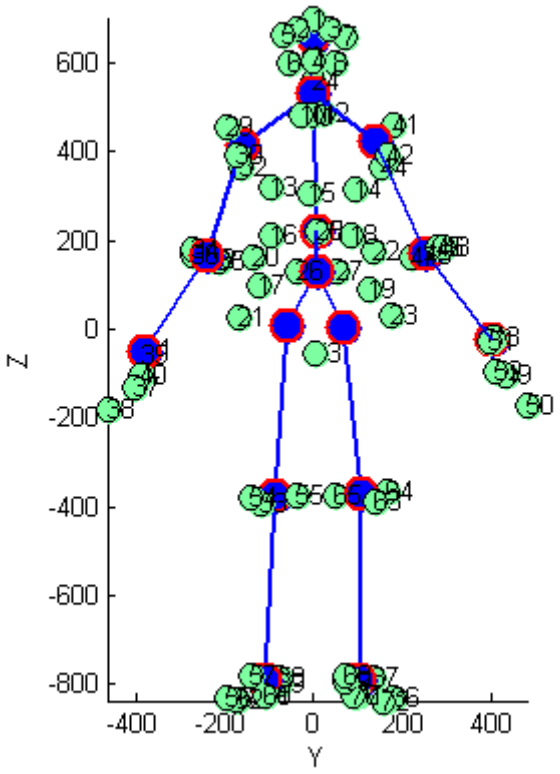

Figure 1. Landmarks, joint centers, and skeleton model

2.2 Skeleton model building

A skeleton model is built by connecting respective joint centers to represent the articulated structure and segments of human body, as shown in **Figure 1**. Note that while the skeleton model thus defined works well for static shape modeling, it may not be suitable for pose changing modeling or dynamic shape modeling, because in the latter cases the joint centers need to describe the true kinematics of human body motion.

2.3 Segmentation

The entire body scan is divided into segments according to the skeleton model with some special treatment in certain body areas, such as the crotch area and the armpit area. In order to automatically segment the surfaces in these particular areas, certain geometric constraints can be applied. Since the surfaces of hands and feet were not scanned in sufficient detail in the CAESAR database, they are excluded from the main body and can be treated separately. Otherwise, generic hand/foot models can be integrated into the main body for the static shape modeling. **Figure 2** illustrates surface segmentation by using difference colors to distinguish them.

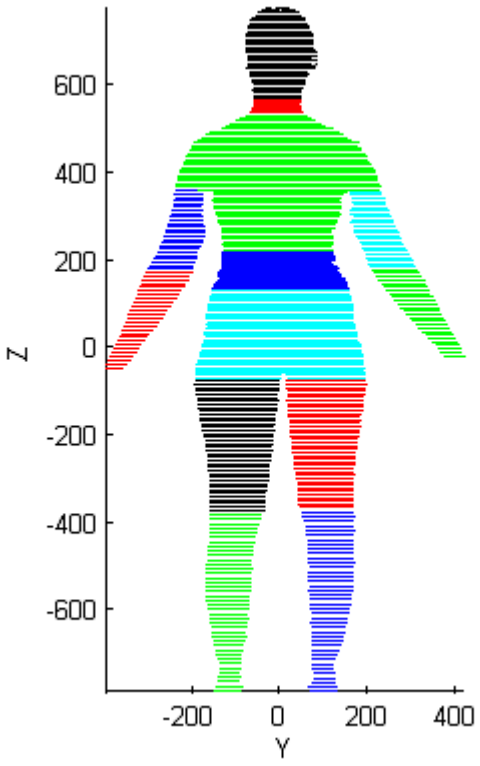

Figure 2. Segmentation and slicing

2.4 Slicing

The scan of each segment is sliced along the main axis of each segment at fixed intervals**,** which produces the contour lines of the segment, as shown in **Figure 2**. The interval length for each segment varies depending upon the surface variation and area.

2.5 Discretizing

Each contour line is discretized with respect to a polar angle. As such, the two-dimensional contour curve is represented by a vector, as shown in **Figure 3**

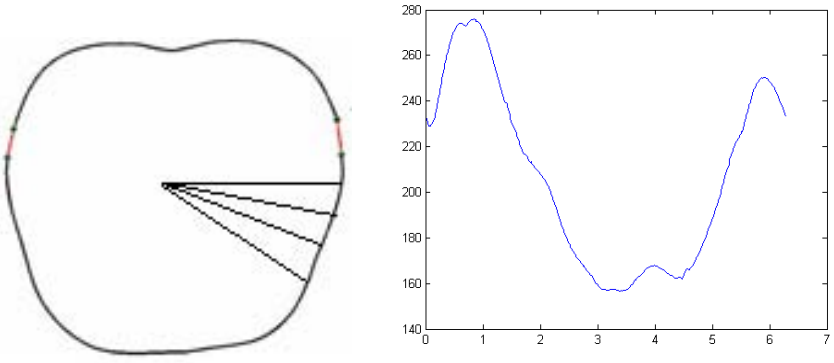

Figure 3. Discretizing contour lines

2.6 Hole filling

The original scan data usually contain holes of various sizes. The hole filling is performed on contour lines for each segment. Different methods were used for three different cases. For a small hole, the gap in a contour line is filled using one-dimensional interpolation. For a medium-size hole, the hole is amended using two-dimensional interpolation on the multiple contour lines containing the hole. For a large hole or surface opening, a piece of surface from a template shape model in the corresponding area is deformed and fitted to patch the hole. **Figure 4** illustrates an example of hole filling based on contour lines.

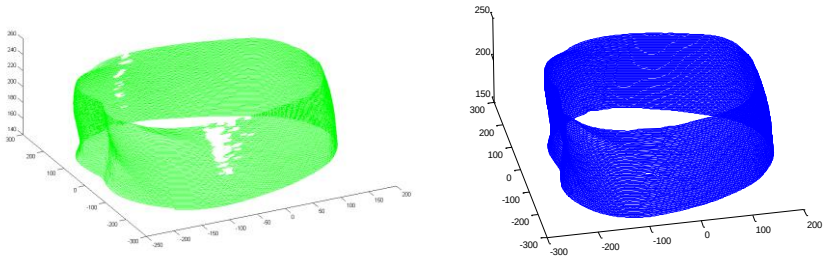

Figure 4. Hole filling

2.7 Parameterization and shape description

The vector of each discretized contour line is combined together to form the total vector that describes the entire body shape. Alternatively, the vector of each discretized contour line can be considered as a signal and decomposed on a wavelet basis. As such, each contour line is represented by a set of wavelet coefficients. The combination of the wavelet coefficients of all contour lines forms a vector that describes the body shape in terms of wavelet coefficients. Since only a few wavelet coefficients are needed to represent the original signal, the dimension of the wavelet coefficient vector will be much smaller than that of the original.

2.8 Surface Registration

After the same schemes of segmentation, slicing, discretizing, and parameterization are applied to different scans (subjects), the point-to-point correspondence among the scans of different bodies is established. This presents a way for surface registration.

2.9 Shape Variation Characterization Using PCA

Principal component analysis (PCA) is a major method often used to characterize human shape variations. Suppose

$$\mathbf{S}_m = \{c_{mn}^{kl}\},\ n = 1, N; k = 1, K; l = 1, L \tag{1}$$

is a shape descriptor , where m=1, ..., M denotes each subject, n=1, …, N points to each segment of a subject, k=1, …, K describes each contour line of a segment, and l=1, …, L refers to each point of a contour line (or each wavelet coefficients if each contour line is expanded in terms of wavelets). Conventional PCA of shape $\mathbf{S}_m$ is described as follows:

$$\begin{aligned}
&\overline{\mathbf{S}}_m = \sum_{m=1}^{M} \mathbf{S}_m \\
&\tilde{\mathbf{S}}_m = \mathbf{S}_m - \mathbf{S}_m \\
&\mathbf{A} = [\tilde{\mathbf{S}}_1 \tilde{\mathbf{S}}_2 \ldots \tilde{\mathbf{S}}_M], \\
&\mathbf{U} = \mathbf{A}\mathbf{A}^T \\
&\mathbf{V}^{-1}\mathbf{U}\mathbf{V} = \mathbf{D}
\end{aligned} \tag{2}$$

where $\mathbf{V}$ contains the eigen vect ors of $\mathbf{U}$ and diag($\mathbf{D}$) are the eigen valu es of $\mathbf{U}$. However, a problem with this approach is that as each $\mathbf{S}_m$ may contain thousands of elements, $\mathbf{U}$ is a matrix with huge size that can easily exceeds the capacity of computer memory.

In order to cope with this problem, a method called incremental principal component analysis (IPCA) can be used. However, it has several potential problems also. Alternatively, a special treatment can be implemented on the conventional PCA. Denote

$$\mathbf{C}' = \mathbf{A}^T\mathbf{A}, \tag{3}$$

as a new covariance matrix with much smaller size (whose dimension equals the number of observations). The eigen values of $\mathbf{C}'$ are given by

$$\mathbf{V}'^{-1}\mathbf{C}'\mathbf{V}' = \mathbf{D}', \tag{4}$$

where $\mathbf{V}'$ contains eigen vectors and diag($\mathbf{D}'$) are eigen values. From Eq. (4) it follows that

$$\mathbf{C}'\mathbf{V}' = \mathbf{D}'\mathbf{V}', \tag{5}$$

that is,

$$\mathbf{C}'\mathbf{v}'_i = d'_i\mathbf{v}'_i, \tag{6}$$

or

$$\mathbf{A}^T\mathbf{A}\mathbf{v}'_i = d'_i\mathbf{v}'_i. \tag{7}$$

Further,

$$\mathbf{A}\mathbf{A}^T\mathbf{A}\mathbf{v}'_i = d'_i\mathbf{A}\mathbf{v}'_i. \quad (8)$$

That is

$$\mathbf{C}\mathbf{A}\mathbf{v}'_i = d'_i\mathbf{A}\mathbf{v}'_i. \quad (9)$$

Let

$$\mathbf{v}_i = \mathbf{A}\mathbf{v}'_i, \quad (10)$$

and

$$d_i = d'_i, \quad (11)$$

Or

$$\mathbf{V} = \mathbf{A}\mathbf{V}' \quad (12)$$

$$\mathbf{D} = \mathbf{D}'. \quad (13)$$

Further, $\mathbf{V}$ needs to be normalized by

$$\mathbf{V} = \mathbf{A}\mathbf{V}' * abs(\mathbf{D}')^{-1/2}. \quad (14)$$

The principal components of $\mathbf{A}$ are given by Eq. (12). Since $\mathbf{C}'$ is usually much smaller than $\mathbf{C}$, the PCA becomes tractable for the capacity of computer memory.

While the body shape variation can be characterized with respect to the entire population, certain features or characteristics are uniquely associated with gender, ethnicity, age, and some other classifiers. Conversely, these unique body features can provide useful clues about a subject of interest. Therefore, PCA can be conducted on particular cases, such as

- Case-1: Overall PCA: all subjects in the database as one group;
- Case-2: Group PCA: subjects grouped according to gender;
- Case-3: Group PCA: subjects grouped according to age band;
- Case-4: Group PCA: Subjects grouped according to ethnicity.

2.10 Feature Extraction with Control Parameters

Principal component analysis helps to characterize the space of human body variation, but it does not provide a direct way to explore the range of bodies with intuitive control parameters, such as height and weight. Allen et al [4] showed how to relate several variables simultaneously by learning a linear mapping between the control parameters and the PCA weights. Ben Azouz et al [5] attempted to link the principal modes to some intuitive body shape variations by visualizing the first five modes of variation and giving interpretations of these modes. Alternatively, sizing parameters or anthropometric measurements can be used to control the body shape. However, providing all measurements that are sufficient to describe a detailed shape model would be almost impractical. Instead, eight anthropometric measurements (5 girths and 3 lengths) were used as sizing parameters in this project, as displayed in Figure 5. These eight primary measurements have been defined as the primary body measurements for product-independent size assignment [6] and were used by Seo et al [7] for human shape synthesizing. Using such a small measurement set provides compact, easily obtainable parameters for the body geometry representation, enabling applications such as an online clothing store, where a user is asked to enter his/her measurements for customized apparel design. Because landmark data were collected and provided in the CAESAR database, these size parameters can be calculated for each subject using landmark data.

Body measurement	Definition
Stature	Vertical distance between the crown of the head and the ground
Crotch length	The vertical distance between the crotch level at center of body and the ground
Arm length	The distance from the armscye shoulder line intersection (acromion) over the elbow to the far end of the prominent wrist bone (ulna) in line with small finger
Neck girth	The girth of the neck-base
Chest/Bust girth	Maximum circumference of the trunk measured at bust /chest height
Under-bust girth	Horizontal girth of the body immediately below the breasts
Waist girth	Horizontal girth at waist height
Hip girth	Horizontal girth of the trunk measured at hip height

(a)

(b)

Figure 5. Control parameters of body shape

The relationship between the control parameters and characterized shape variations can be established via linear mapping. Denote

$$\mathbf{q_i} = \{q_1\, q_2 .. q_M\, 1\}^T, \tag{15}$$

as the control parameters of a subject shape,

$$\mathbf{p_i} = \{p_1\, p_2 ... p_N\}, \tag{16}$$

as the projection coefficients in the eigenspace (PCA weights). Then the relationship can be expressed as

$$\mathbf{p_i} = \mathbf{M}\mathbf{q_i}, \tag{17}$$

where $\mathbf{M}$ is a $N \times (M+1)$ mapping matrix. Equation (17) represents a linear relation. However, nonlinear relationship can also be considered. Suppose Eq. (17) applies to all subjects under survey. Then

$$[\mathbf{p_1}\, \mathbf{p_2} ... \mathbf{p_K}] = \mathbf{M}[\mathbf{q_1}\, \mathbf{q_2} .. \mathbf{q_K}], \tag{18}$$

which can be solved using the least squares method.

2.11 Shape Reconstruction/Morphing

Given a number of scan data sets of different subjects, a novel human shape can be created that will have resemblance to the samples but is not the exact copy of any existing shapes. This can be realized via reconstruction and morphing. Four methods were developed for shape reconstruction and morphing.

2.11.1 Morphing between two examples

Morphing between any two subjects' scans can be done by taking linear combinations of their vertices. In order to create a faithful intermediate shape between two individuals, it is critical that

all features are well-aligned; otherwise, features will cross-fade instead of morphing. **Figure 7** illustrates the morphing from a male subject to a female subject after the surfaces from both subjects were registered.

2.11.2 Interpolation in a multi-dimensional space

Given a set of shape models of different subjects $\{S_i\}$, collectively they define a multi-dimensional space where each model S_i represents a separate axis space and is assigned to a location in the dimension space, d_i. The goal is to produce, at any point d in the space, a new shape model that is derived through the interpolation of the example shape models. When d is equal to the position d_i for a particular example model S_i, then $S(d)$ should be equal to S_i, which is the shape of example i. Between the examples, smooth intuitive changes should take place. This means that a new model in between will merge the features from all example models in the space rather than just two adjacent to it, as in the preceding case. This can be considered as a problem of multi-dimensional scattered data interpolation. A common approach to the problem is to use Gaussian radial basis functions (GRBFs), which we will use for the multi-dimensional interpolation.

2.11.3 Reconstruction from Eigen space

After PCA analysis, the features of sample shapes are characterized by eigenvectors or eigen persons which form an eigen space. Any new shape model can be generated from this space by combining a number of eigen models with appropriate weighting factors.

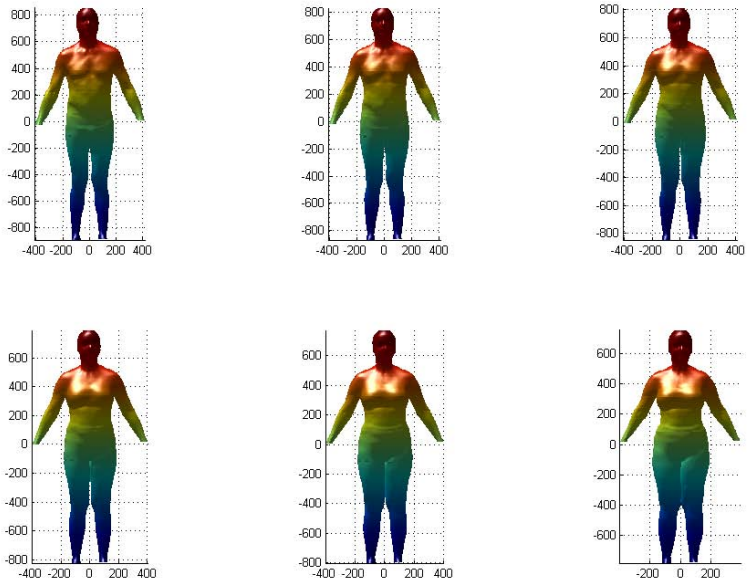

Figure 7. Morphing from a male to a female

2.11.4 Feature-based Synthesis

Once the relationship between human anthropometric features and eigenvectors is established, a new shape model can be constructed from the eigen space with desired features by editing multiple correlated attributes (e.g., height and weight, or other body size parameters). In particular, a semantic structure, as shown in Figure 8 can be used for shape reconstruction. This scheme will allow us to derive a realistic model with different resolutions using information from different sources at different levels. The technique can be used in the visualization of multi-modality data.

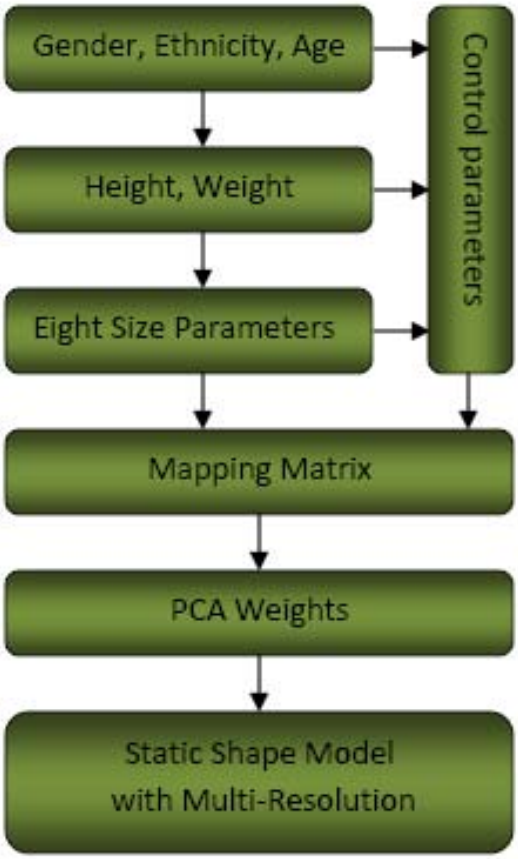

Figure 8. A semantic structure for shape reconstruction

2.12 Part blending

In certain areas where two segments merged together, part blending may be necessary in order to attain a smooth surface transition and a realistic surface representation. Part blending becomes more important in pose modeling and dynamic modeling where surfaces (skins) in joint areas are usually subject to large deformations.

3.0 HUMAN SHAPE MODELING IN VARIOUS POSES

3.1 Problem Analysis and Approach Formation

In order to develop feasible and effective pose modeling methods, a general analysis of the problem is in order.

- The human body is an articulated structure. That is, the human body can be treated as a system of segments linked by joints.
- The human pose changes as the joints rotate. Therefore, a pose can be defined in terms of respective joint angles.
- The body shape varies in different poses. The variations are caused by two factors: the articulated motion of each segment and the surface deformation of each segment.
- It can be reasonably assumed that the surface deformation of a segment depends only on the rotations of the joint(s) adjacent to the segment. While the surface deformation of certain body regions may still be affected by the rotations of joints that are not directly connected, this assumption is valid for most regions of the human body and thus is often used.

Based on the above analyses, a framework for pose modeling was formulated, as shown in Figure 9. The core part of pose modeling is to establish a mapping matrix that can be used to predict and construct the body shape model of a particular person at a particular pose. Therefore, in the true meaning of pose modeling, the mapping matrix needs to represent the shape changes not only due to body variations of different human and pose deformations at different poses independently, but also resulting from the cross correlations between identity and pose. In reality, it is not feasible to determine the relationship between the pose deformation and the body shape variation using PCA in the same way as used for shape variation analysis, since it is too costly to collect pose data for a large number of subjects. Alternatively, it is possible to collect pose data for several typical subjects (e.g., male, female, tall, short, big, and small) who are selected to represent the entire population. For a particular subject, the mapping matrix for his/her pose deformation can be determined by subject classification based on certain criteria such as nearest neighborhood.

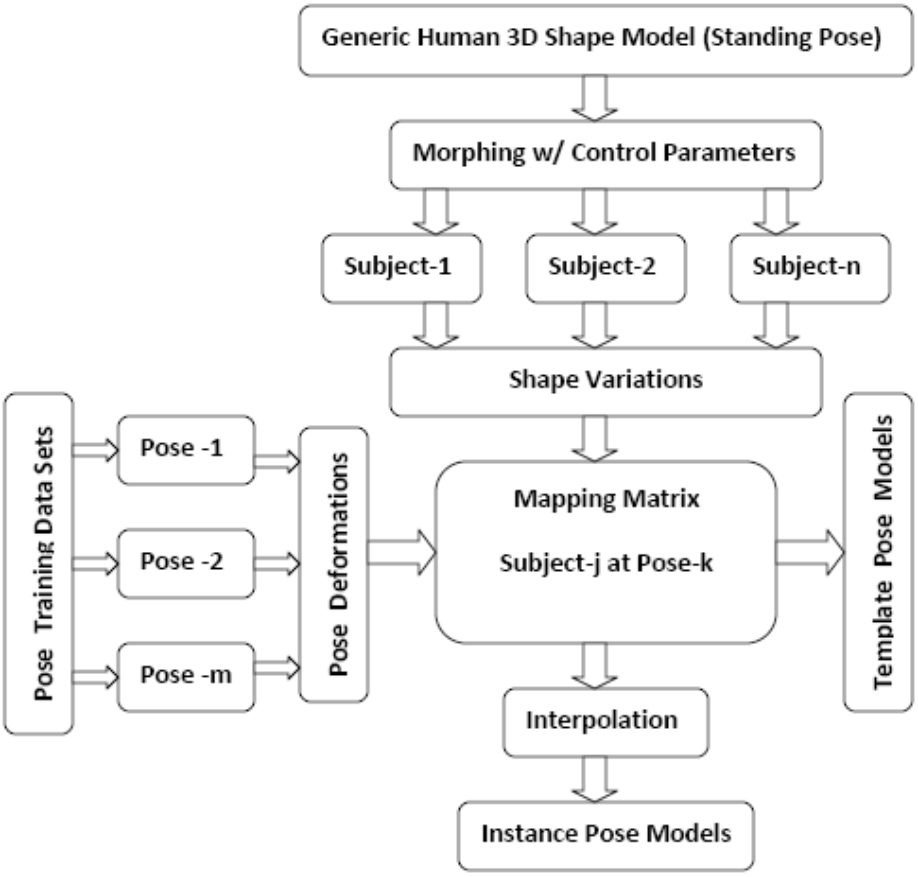

Figure 9. The framework of a pose modeling technology

3.2 Data Collection and Processing

In order to create a morphable (for different subjects), deformable (for different poses), 3-D model of human body shape, it is necessary to collect many samples of human shape and pose. Properly sampling the entire range of human body shapes and poses is important to creating a robust model. The CAESAR (Civilian American and European Surface Anthropometry Resource) database provides human shape data for thousands of subjects in three poses. It can be used to train a static shape model and to represent human shape variation. The data sets that are required to establish a pose mapping matrix and to train pose models are not publicly available. The data used in this research, however, was collected by Anguelov et al [8] from one subject in 70 poses.

In order to use the pose data for pose modeling, data processing is usually required. It includes three major tasks: hole-filling, point-to-point registration, and automatic surface segmentation.

- *Hole-filling* Polygonal meshes that are derived from laser scanners frequently have missing data for regions where the laser neither reached nor produced adequate reflectance. This problem occurs more often when a subject is not in the standard pose (the standing pose used

in the CAESAR database). Interpolating data into these regions often goes by the name of hole-filling. Several methods have been developed for hole-filling, such as the volumetric method [9].

- *Point-to-point registration* Polygonal mesh surfaces of the same object, but taken during different scans are not naturally in correspondence. In order to form complete models it is necessary to find this correspondence, i.e., which point on surface A corresponds to which point on surface B. Non-rigid registration is required to bring 3-D meshes of people in different poses into alignment. While many academic papers have been published which describe fully automated methods [10, 11], the complexity of the problem often leads to optimization prone to local minima. Thus most of these methods tend to lack sufficient robustness for unattended real world applications. Fortunately, establishing correspondence of a few control points by hand is usually sufficient to insure convergence. Labeling more points insures better convergence.

- *Automatic surface segmentation* Given a deformable surface with multiple poses brought into correspondence, it is possible to segment the surface into disjoint regions. Each of these regions approximates a rigid articulated segment of the human body [12, 13]. The easiest way to achieve segmentation is to observe that polygons in the same segment tend to move together, that is, their rotation and translation are the same for a given pair of poses. By performing a K-means clustering over all polygons in all poses, and enforcing continuity of segments, the best segmentation is obtainable.

3.3 Pose Deformation Modeling

The template model associated with the pose dataset consists of 16 segments, each of which has the pre-defined surface division, as shown in Figure 10 [8]. Identifying the surface for each segment in different poses and establishing point-to-point correspondence for each surface in all observed poses is essential to the pose modeling. The method developed for pose deformation modeling in this paper consists of multiple steps, which are described below.

Figure 10. A template model for pose modeling

3.3.1 Coordinate Transformation

The body shape variations caused by pose changing and motion can be decomposed into rigid and non-rigid deformation. Rigid deformation is associated with the orientation and position of segments. Non-rigid deformation is related to the changes in shape of soft tissues associated with segments in motion, which, however, excludes local deformation caused by muscle action alone. In the global (body) coordinate system, a segment surface has the articulated motion and surface deformation. However, in the local (segment) coordinate system, a segment surface has deformation only. Therefore, by transforming the global coordinate system to the local system, the effect of the articulated motion on each segment could be eliminated.

Denote $\mathbf{S}_{jL}$ as the vector of surface vertices in the local coordinate system and $\mathbf{S}_{jG}$ as the vector in the global system, the transformation from the global to the local is given by

$$\mathbf{S}_{jL} = \mathbf{T} \bullet (\mathbf{S}_{jG} - \mathbf{C}_j), \tag{19}$$

where $\mathbf{T}$ is the transformation matrix from the global to the local, and $\mathbf{C}_j$ is the center of gravity of segment –j.

The principal axes of the entire body are used to define the global (body) coordinate system and the principal axes of each segment are used to define the local (segment) coordinate system. The calculation of principal axes is given by the following equations.

$$m_{pqr} = \iiint_M x^p y^q z^r f(x,y,z) dxdydz, \tag{20}$$

where $f(x,y,z)$ is the area of a triangle and (x,y,z) denote the middle point of the triangle. The center of gravity of a surface is given by

$$\mathbf{C} = [m_{110}, m_{010}, m_{001}]^T. \quad (21)$$

Denote

$$\mathbf{U} = \begin{bmatrix} m_{200} & m_{110} & m_{101} \\ m_{110} & m_{020} & m_{011} \\ m_{101} & m_{011} & m_{002} \end{bmatrix}, \quad (22)$$

as the inertial tensor. Then,

$$\mathbf{T}^{-1}\mathbf{U}\mathbf{T} = \mathbf{D}, \quad (23)$$

representing the eigenvalue decomposition of $\mathbf{U}$, where $\mathbf{T}$ contains the eigenvectors of $\mathbf{U}$ and diag($\mathbf{D}$) are the eigenvalues of $\mathbf{U}$.

3.3.2 Surface Deformation Characterization

Suppose the surface deformations of each segment are collected in all poses. Then PCA can be used to find the principal components of the surface deformation for each segment. Collect the surface deformations of each segment in all poses. That is,

$$\mathbf{A} = [\mathbf{S}_{j1L}\, \mathbf{S}_{j2L} \ldots \mathbf{S}_{jNL}], \quad (24)$$

where N is the number of poses under observation. Then the PCA defined by Eqs. (3)-(13) can be used to find the principal components of the surface deformation for each segment. As the PCA exploits the underlying characteristics of the data sets **A**, the surface deformation of a segment in all poses can be characterized by these principal components.

Figure 11 illustrates the eigen value percentage ratio in each component (total 70) of all segments (total 16). It is shown that for all segments, the variance (eigen value ratio) of principal components increases sequentially, and significant principal components are those from the order of 60 to 70. As PCA exploits the underlying characteristics of a data set, the surface deformation of a segment in all observed poses can be characterized by these principal components. The surface deformation in a particular pose can be decomposed or projected in the space that is formed by the PCs. Each decomposition/projection coefficient represents the contribution or effect from the corresponding PC.

The decomposition or projection of the surface deformations of a segment in all poses in the eigen space is given by

$$\mathbf{P} = \mathbf{A}'\mathbf{V}. \quad (25)$$

Each column of $\mathbf{P}$ contains the decomposition/projection coefficients of the surface deformation in each corresponding pose.

These coefficients can be used to reconstruct the surface deformation. There are two types of reconstruction.

- Full reconstruction, which, using all the PCs or eigenvectors, is given by

$$\mathbf{A} = \mathbf{V}\mathbf{P}'. \quad (26)$$

It is shown that the full reconstruction can completely reconstruct the original surface deformation. Thus it is a perfect reconstruction.

- Partial reconstruction, which, using a number of significant PCs, is given by

$$\tilde{\mathbf{A}} = \tilde{\mathbf{V}}\tilde{\mathbf{P}}', \tag{27}$$

where $\tilde{\mathbf{V}}$ contains significant principal components, and $\tilde{\mathbf{P}}$ contains the coefficients corresponding to these components.

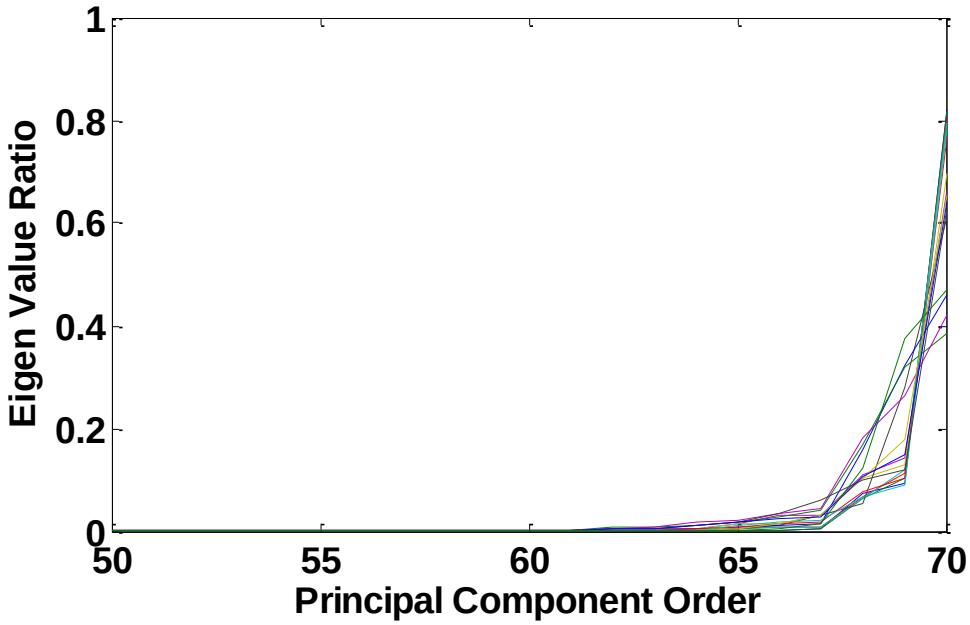

Figure 11. Eigen value ratio for all 16 segments

Figure 12 illustrates the reconstructed shape for 2 different poses. In each row of Figure 12, the first is the original shape, the second is the shape from full reconstruction, and the third and fourth are the shapes from partial reconstruction with 20 and 10 largest PCs, respectively. Figure 13 displays the sum of square errors of surface vertices for full and partial reconstruction. It is shown that the full reconstruction can completely reconstruct the original surface deformation in all poses, which means it is a perfect reconstruction, and partial reconstruction can provide a reasonable approximation of the original shape. While full reconstruction provides complete reconstruction of the original deformation, it is not necessary in many cases. On the other hand, the accuracy of partial reconstruction can be controlled by selecting a proper number of significant PCs. As partial reconstruction provides a reasonable simplification or approximation to the original deformation, it is often used in practice.

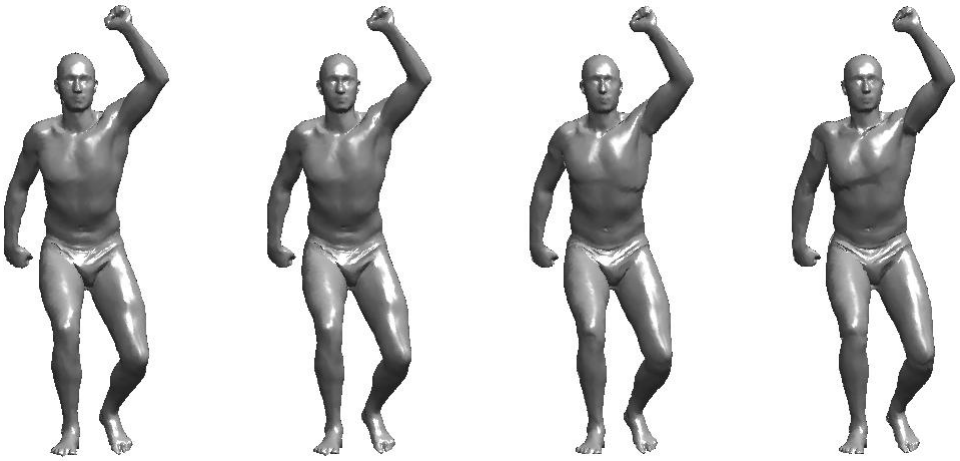

(a) Pose-1

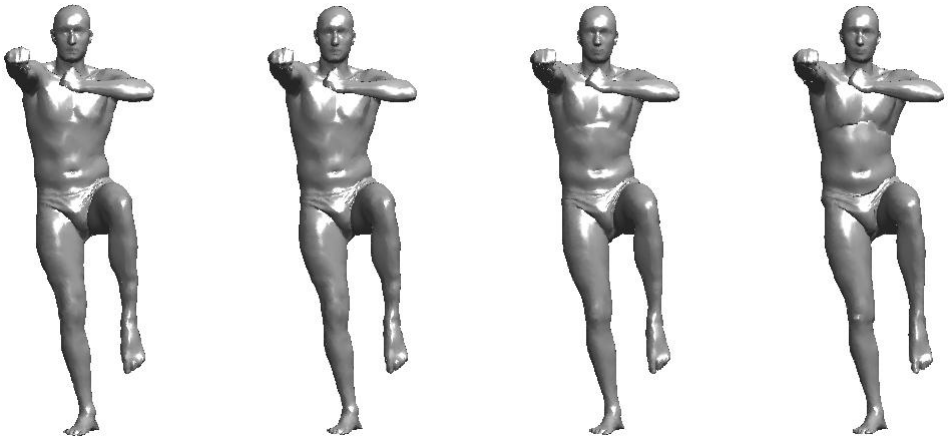

(b) Pose-2

Figure 12. Shape reconstruction using principal components

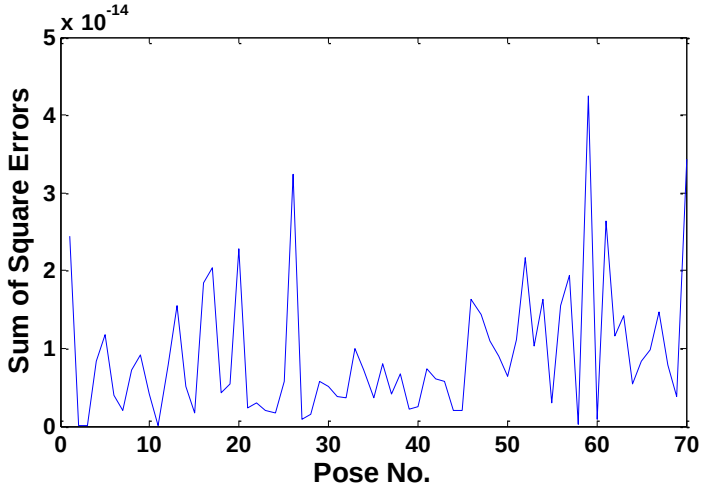

(a) Full reconstruction

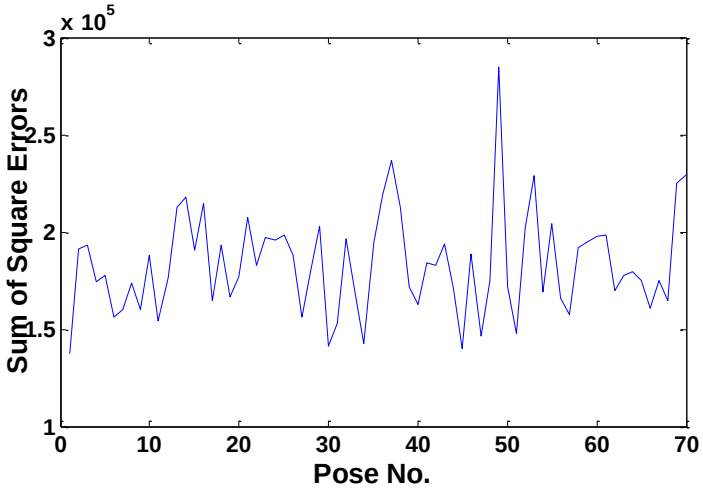

(b) Partial reconstruction with 20 largest PCs

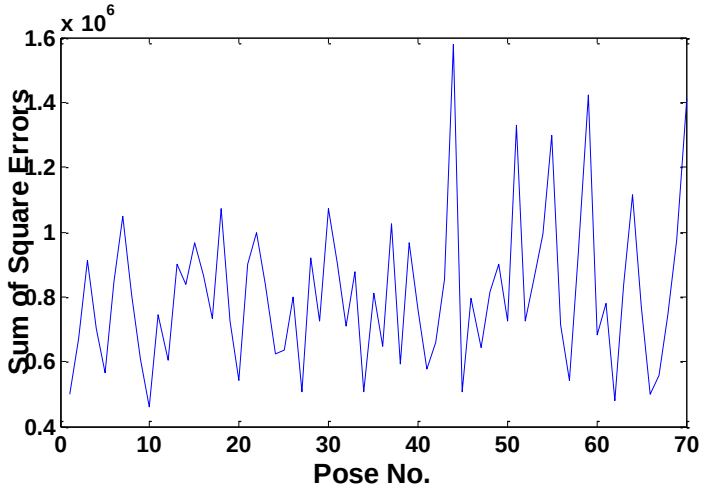

(c) Partial reconstruction with 10 largest PCs

Figure 13. Sum of square errors of shape reconstruction

3.3.3 Surface Deformation Representation

As the surface deformation of a segment is assumed to depend only on the rotation of the joint(s) connected, the relationship between the surface deformation and joint rotations has to be known. Joint rotations can be conveniently represented by their twist coordinates, which in turn can be described by a vector $\mathbf{t}$. The surface deformation can be compactly represented by its decomposition or projection coefficients in the eigen space given by Eq. (25). Ideally, the surface deformation can be expressed as a function of joint rotations:

$$\mathbf{S}_{pi} = S(\mathbf{t}), \quad (28)$$

where $\mathbf{S}_{pi}$ represents the surface deformation in a particular pose. The relation represented by Eq. (28) can be linear or nonlinear. An appropriate function needs to be identified for Eq. (28). The same function of Eq. (28) can be applied to all poses. Then, the measurement of surface deformation and joint rotations in all poses can be used to estimate the parameters of $S(\mathbf{t})$.

3.3.4 Surface Deformation Prediction

It is not feasible to measure the surface deformation of each segment for all possible poses, because the human body has a large number of degrees of freedom and can virtually make an infinite number of different poses. As a matter of fact, only a limited number of poses can be investigated in tests, but it is often required to predict surface deformation for new poses that have not been observed. Three methods can be used to predict surface deformation.

- *Method-1*: using principal components. Given joint twist angles {**t**} for a segment to define a particular pose i, projection coefficients {**P**i} can be estimated using Eq. (25). Using a full or partial set of principal components {**v**}, the surface deformation is reconstructed.
- *Method-2*: taking nearest neighbor pose. Given the joint twist angles {**t**} for a segment to define a particular pose i, find the nearest neighbor to the prescribed pose and take its surface deformation as an approximation. The neighborhood is measured in terms of the Euclidean distance between the joint twist angles for the two poses.
- *Method-3*: interpolating between two nearest neighbors. Given the joint twist angles {**t**} for a segment to define a particular pose i, find the two nearest neighbors to the prescribed pose, The pose deformation is determined by interpolating between the deformations of these two neighbor poses.

3.3.5 Body Shape Prediction for New Poses

The body shape for a new pose can be predicted following a procedure as follows:

- Define a body pose by prescribing joint twist angles for each segment;
- Determine from joint angles the orientation and position of each segment in the global (body) coordinate system;
- Determine the surface deformation of each segment;
- Obtain the segment surface by adding the surface deformation to its mean shape;
- Transfer each segment surface from the local coordinate system to the global system by

$$\mathbf{S}_{jG} = \mathbf{T}^{'} \bullet \mathbf{S}_{jL} + \mathbf{C}_{j}. \quad (29)$$

Figure 14 illustrates the predicted shape for 8 different poses using method-2.

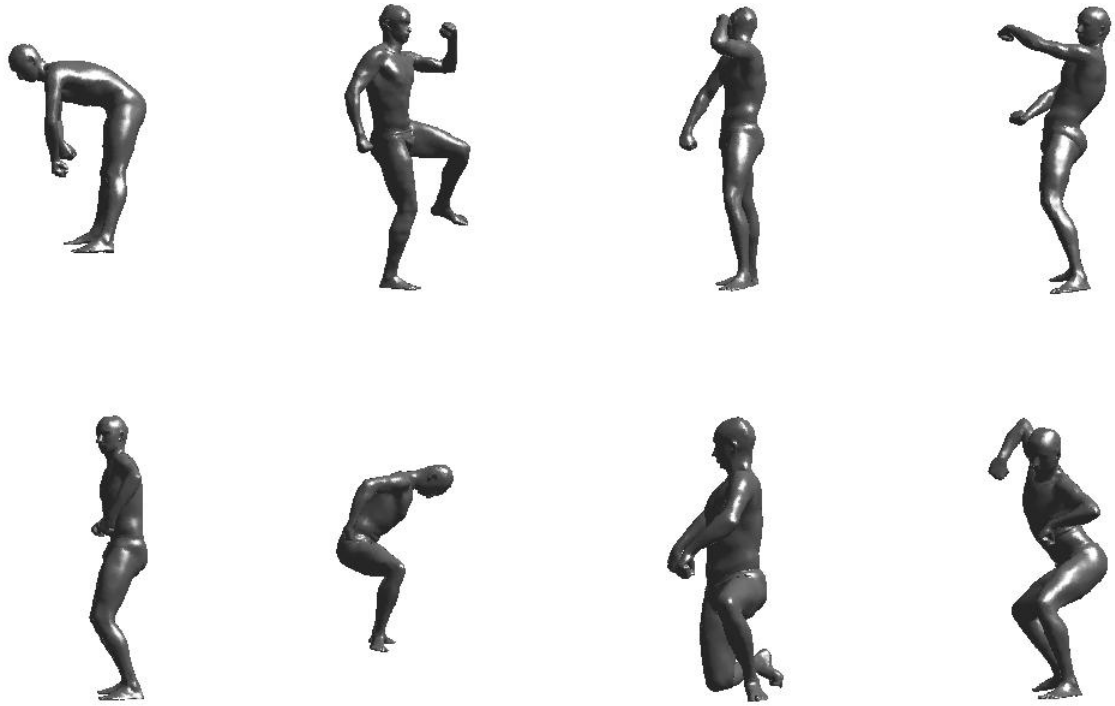

Figure 14. Predicted shape in 8 different poses

4.0 DYNAMIC MODELING

4.1 General Considerations

While the human body is moving, changing poses, or performing actions, the status is referred to as human in motion. The shape of the body changes while the human is in motion. Dynamic modeling describes or captures the body shape changes while the human is in motion. Dynamic human shape modeling is a challenging topic because (a) the human can take various poses; (b) video imagery provides an incomplete view of the body due to segment occlusion; and (c) video imagery is often contaminated with noise due to changing of light, view point/angle, etc. However, since the human is in motion, video imagery could capture the human body from different viewing angles even if only one camera is used. Therefore, given a multi-viewpoint video record, if the capture time is long enough, it can be reasonably assumed that: (a) the subject exposed every part of the body to the camera (in a common sense); and (b) the subject took all poses associated with the activity played. Robust and efficient dynamic modeling needs to use the information contained in each frame of video imagery and to fuse the information obtained from all frames. As such, dynamic modeling will be more capable of capturing the human body shape and detecting human intention.

A strategy for dynamic modeling is illustrated in Figure 15. It uses 2-D video imagery as the input and provides a dynamic model as the output. Dynamic modeling is treated as an iterative process that consists of multiple steps. The details of the scheme are described as follows.

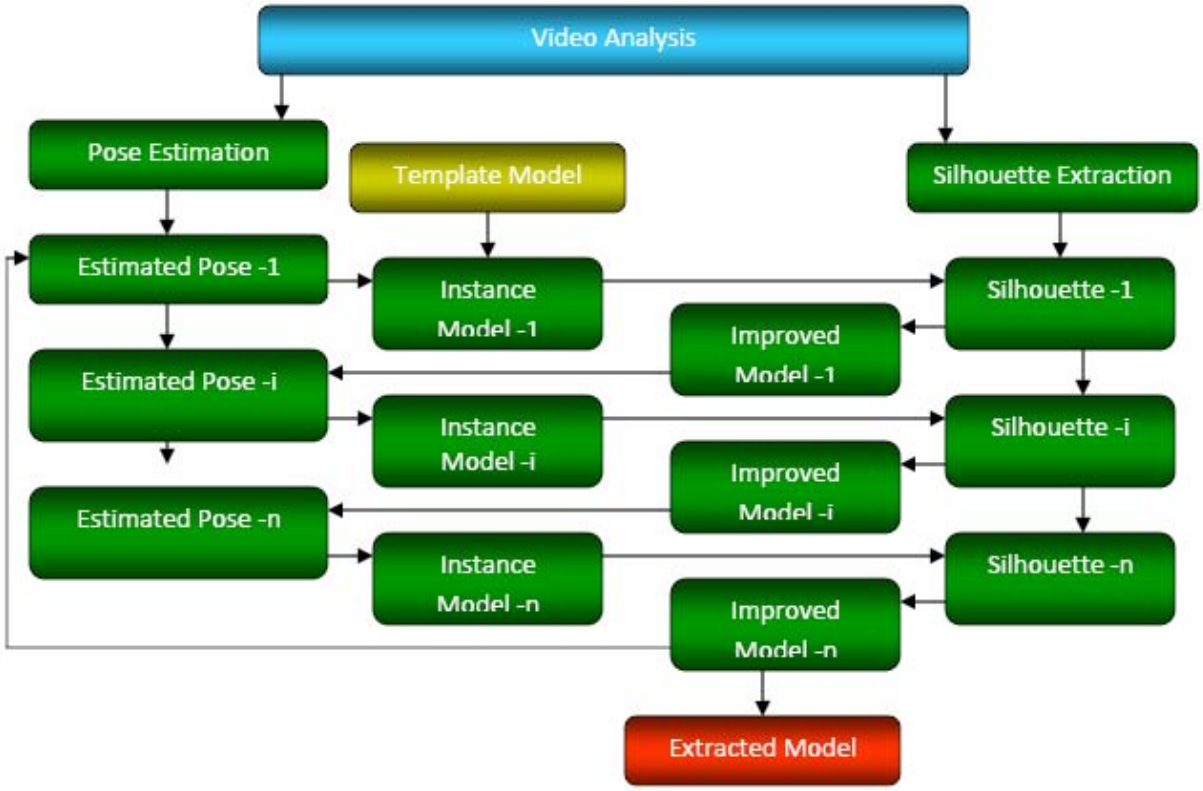

Figure 15. A scheme for dynamic modeling

4.2 Template Model

A template model is a base model that provides a complete, fundamental structure for human shape modeling. In order for a template model to be usable for dynamic shape modeling, it needs to be parameterized and capable of dealing with the shape variation among different subjects and the shape deformation in various poses. Such a model can be created by integrating static shape modeling (shape descriptor, principal components, and shape control parameters) with pose modeling (pose definition, pose-dependent surface deformation, and pose control parameters). There are two models of this kind. One is the SCAPE (Shape Completion and Animation of People) developed by Anguelov et al [8]. The other model is the statistic model of human pose and body shape developed by Hasler et al [14].

The pose modeling technology described in Figure 9 is segment-based. It treats the surface of each segment as a whole, uses PCA to characterize the surface deformation, and handles the coupling effect between shape variations and pose deformations. It is unique and can create a template model that meets the needs from dynamic shape modeling.

4.3 Instance Model

An instance model is the model constructed from the template model for the subject in a particular pose (corresponding to a particular video frame). In order to generate the first instance model, semantic shape reconstruction scheme (Figure 8) can be implemented to use any shape information available (from gender, race, and age to size parameters). If none of these data are provided, a generic shape model (a 50^{th} % male, for example) can be generated. For the instance models in the subsequent poses (frames), the shape information comes from the optimization (fitting) in the previous step. The pose information for each instance model in the first iteration is provided by video analysis. In the subsequent iterations, the pose information for each instance model is provided by the fitted model in the previous iteration at the same frame.

4.4 Model fitting

Each instance model provides a set of initial values for the control parameters of the model, which are usually not good enough for the description of the ground truth of the shape. The estimation of the parameters of the true model is done by fitting the projection of the instance model to the silhouette extracted from video imagery. The problem of model fitting can be formulated as an optimization problem.

Denote

$$\mathbf{p}_m = \{\boldsymbol{\beta}^T \, \boldsymbol{\alpha}^T\}^T, \tag{30}$$

as the vector of model parameters, where

$$\boldsymbol{\beta} = \{\beta_1 \, \beta_2 \ldots \beta_n\}^T, \tag{31}$$

as the control parameters for the shape variation and

$$\boldsymbol{\alpha}^T = \{\alpha_1 \, \alpha_2 \ldots \alpha_m\}^T, \tag{32}$$

as the control parameters for the pose-dependent surface deformation. Then, from the template model,

$$\mathbf{S} = S(\mathbf{p}_m), \tag{33}$$

which is a shape descriptor vector and represents the shape model corresponding to control parameters $\mathbf{p}_m$.

For a given camera view, a foreground silhouette F^I, which extracts the subject from background, is computed using standard background subtraction methods. The hypothesized shape model is projected onto the plane which is defined by F^I:

$$F^M = P(\mathbf{S}, \boldsymbol{\gamma}), \tag{34}$$

where $\boldsymbol{\gamma}$ is the parameter related to camera view which may or may not be known. The projection F^M can be considered as the estimated silhouette in the same frame. The extraction of a dynamic model from video imagery can be conducted by fitting F^M to F^I for a sequence of image frames where the method proposed by Balan et al [15] can be used. The cost function is a measure of similarity between two these silhouettes. For a given camera view, a foreground silhouette F^I is computed using standard background subtraction methods. This is then compared with the model silhouette F^M. The pixels in non-overlapping regions in one silhouette

are penalized by the shortest distance to the other silhouette [16] and vice-versa. To do so, a Chamfer distance map [17] is computed for each silhouette, C^M for the hypothesized model and C^I for the image silhouette. This process is illustrated in Figure 16. The predicted silhouette should not exceed the image foreground silhouette (therefore minimizing $F^M C^I$), while at the same time trying to explain as much of it as possible (thus minimizing $F^I C^M$). Both constraints are combined into a cost function that sums the errors over all image pixels px:

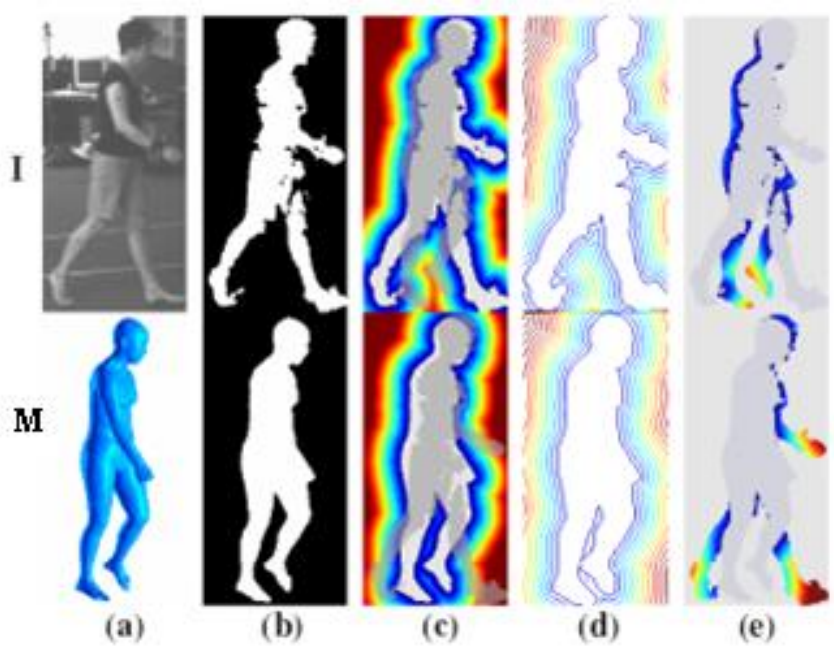

Figure 16. Cost function

(a) original image I (top) and hypothesized mesh M (bottom); (b) image foreground silhouette F^I and mesh silhouette F^M, with 1 for foreground and 0 for background; (c) Chamfer distance maps C^I and C^M, which are 0 inside the silhouette; the opposing silhouette is overlaid transparently; (d) contour maps for visualizing the distance maps; (e) per pixel silhouette distance from F^M to F^I given by $\sum_{px} F^M_{px} C^I_{px}$ (top), and from F^I to F^M given $\sum_{px} F^I_{px} C^M_{px}$ (bottom).

$$f(\mathbf{p}) = \frac{1}{|px|} \sum_{px} (\delta F^M_{px} C^I_{px} + (1-\delta) F^I_{px} C^M_{px}), \tag{35}$$

where

$$\mathbf{p} = \{\mathbf{p}_\mathbf{m}^\mathbf{T} \ \boldsymbol{\gamma}\}^T, \tag{36}$$

including the control parameters of the model and the parameters related to camera view, and δ weighs the first term more heavily because the image silhouettes are usually wider due to the

effects of clothing. When multiple views are available, the total cost is taken to be the average of the costs for the individual views.

Now, model fitting can be formulated as an optimization as follows:

$$\begin{aligned} &\text{Design variables}: \mathbf{p} \\ &\text{objective function}: \text{Min}\{f(\mathbf{p})\}, \\ &\text{Constraints}: \mathbf{p}^L \le \mathbf{p} \le \mathbf{p}^U \end{aligned} \tag{37}$$

where $\mathbf{p}^L$ and $\mathbf{p}^U$ are lower and upper bounds on the design variables, respectively. The problem of Eq. (33) is nonlinear. While various methods are available for solving Eq. (37), local minima and non-convergence are expected to be common problems.

4.5 Iteration

Usually, the information contained in one frame is not enough to extract a decent model. In other words, model fitting in one pose (frame) will not be able to provide good estimates of all parameters. Local minima and non-convergence may lead to the failure of the optimization at a particular frame. Therefore, an iterative procedure was devised to use the information contained in a sequence of frames and to improve the model fitting (parameter estimation) progressively. As shown in Figure 15, the model fitting is performed on a sequence of frames. Not all the images in consecutive frames will be used in the model fitting. Only those that can provide a sound estimation of pose and are sufficiently distinct from the previous ones will be used for the model fitting. After creating an initial instance model, the estimated model parameters at step i will be used to create the instance model for step i+1, in combination with the pose estimation at step i+1. If the optimization at step i fails, the estimated model parameters from step i-1 will be used to create the instance model for step i+1, with a certain perturbation incorporated. After all the frames in the sequence have been run through, the estimated model parameters at the last step will be used to create the instance model for the first step in the new run. The iteration will repeat until certain tolerances for errors are met.

4.6 Computation Efficiency

It was shown that dynamic model fitting is a time consuming process [15]. As an iterative procedure is to be used to improve model fitting, computational efficiency becomes more important. In particular, the optimization used in model fitting will incur extensive computation as numerous times of 3-D mesh reconstruction and 3-D model projection will be called. In order to perform dynamic modeling in real-time or in nearly real-time, the following measures will be taken to increase computational efficiency.

- Using graphics hardware for the projection of 3-D meshes and the computation of the cost function;
- Implementing parallel computing using CUDA, a parallel computing architecture from NVIDIA. As a general purpose parallel computing architecture, CUDA leverages the parallel computational engine in graphics processing units (GPUs) to solve many complex computational problems in a fraction of the time required on a CPU. It includes the CUDA Instruction Set Architecture (ISA) and the parallel computational engine in the GPU. To program to the CUDA architecture, developers can use C, FORTRAN, C++, and MATLAB.

- Implementing distributed computing to exploit the computing power of a multi-node cluster workstation. Distributed computing often requires parallel schemes. This will greatly enhance our computational capability. In order to attain the goal of real-time dynamic modeling, the implementation of parallel, distributed computing is necessary.

5.0 REPLICATION AND ANIMATION

5.1 Replication

Replication means replicating human motion, actions, and activities captured or recorded by video cameras. It is not simply replaying of video records. A dynamic human shape model can be used to replicate human motion, actions, and activities in 3-D space. Such an example is shown in Figure 17.

5.2 Animation

Realistic human representation and animation remains a primary goal of computer graphics research. Mesh-based methods [18] and skeleton-based methods [7] are two approaches for animation. In fact, a human activity or action can be decomposed into a time-based sequence of frames. In each frame, the human body takes a particular pose. Therefore, the animation of an action/activity can be realized via reconstructing the human shape at each pose (frame). Two methods are developed for the animation using motion capture data.

(a)

(b)

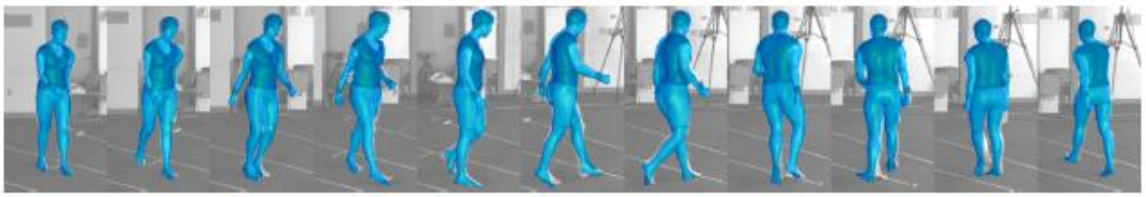

Figure 17. An example of replication
(a) Original video record; and (b) Replication with 3-D dynamic models

5.2.1 Using marker data directly

Motion capture data in the original format provides a 3-D spatial trajectory of each marker. At each frame, these markers provide information about the subject's body shape (as the markers are placed on the body) and the subject's pose in this frame (as the markers move with the body segments). The information can be used to reconstruct a model with both shape and pose information represented. Denote

$$\hat{\mathbf{m}}_j = \{m_{1x}\, m_{1y}\, m_{1z}\, m_{2x}\, m_{2y}\, m_{2z} \ldots m_{nx}\, m_{ny}\, m_{nz}\}^T, \tag{38}$$

as the coordinate vector of the markers at frame j. We use control parameters $\mathbf{p}_m^j$ to create a model mesh at this frame, $\mathbf{S_j}$, which is given by

$$\mathbf{S_j} = S(\mathbf{p}_m^j). \tag{39}$$

From this model, we can calculate the coordinates of the points corresponding to the markers, which are denoted as $\tilde{\mathbf{m}}_j$. The reconstruction of the model is to find a set of parameters $\mathbf{p}_{mo}^j$ such that points $\tilde{\mathbf{m}}_j$ get as close to markers $\hat{\mathbf{m}}_j$ as possible. This can be formulated as an optimization problem:

$$\begin{aligned} &\text{Design variables}: \mathbf{p}_m^j \\ &\text{Objective function}: \text{Min} \left\| \tilde{\mathbf{m}}_j - \hat{\mathbf{m}}_j \right\|. \\ &\text{Constraints}: \mathbf{p}_m^L \le \mathbf{p_m^j} \le \mathbf{p}_m^U \end{aligned} \tag{40}$$

As such, the shape and pose are captured simultaneously. Note that, in many motion capture systems, the markers protrude from the body, so that a reconstructed mesh that achieves the exact marker positions observed may contain unrealistic deformations. In order to avoid these unrealistic shapes and deformations, the model is constrained to lie within the space of body shapes encoded by PCA models. The sequence of meshes (models) produced for the different frames can be strung together to produce a full 3-D animation of the motion capture sequence. Such an example is shown in Figure 18 [8].

Figure 18. An example of marker-based animation

5.2.2 Using joint angles

Based on the motion capture data, joint angles can be calculated for each frame, which can be done in many motion capture systems, such as the one in the 3-D HSL (3-D Human Signatures Laboratory) of the U.S. Air Force Research Laboratory. Based on a specified skeleton model, joint angles can be used to define a pose. From joint angles, a set of control parameters can be derived to create surface deformations that correspond to the pose. The information from the original subject if available, from other subjects as desired, or from a generic human can be used for shape control parameters. Integrated with pose deformations, a complete model is created for

each pose (frame). A sequence of models is strung together to provide an animation that corresponds to the motion sequence. This method will allow us to create virtual activity or replicate human motion in 3-D space, such as that shown in Figure 19.

Figure 19. Human motion replication in 3-D space/Virtual activity creation

6.0 CONCLUDING REMARKS

Extensive investigations were performed in this project on human shape modeling from the perspectives of static shape modeling and morphing, human shape modeling in various poses, dynamic modeling, and human activity replication/ animation. The following conclusions can be made from these investigations.

1. The method developed in this project for static shape modeling and morphing is based on contour line slicing and discretization. This method works well on the body scan data sets (e.g., CAESAR database) where landmarks are available for surface segmentation. It can effectively handle surface registration, parameterization, and approximation. It can be easily used in shape variability analysis. However, it may not be the optimal choice for pose modeling and dynamic modeling where large surface deformation may cause large distortion or folding for contour lines. It may also not be suitable for the body shape data that are acquired without landmarks placed, even though several methods can be used to identify landmarks from surface data.
2. The framework developed in this project for the shape modeling in various poses deals with the coupling between the shape variation among different subjects and the surface deformation in different poses, which is neglected by many existing pose modeling methods. The method developed in this project for surface deformation modeling and characterization is unique, which treats the entire body surface deformation in terms of segment surface deformation, separates the surface deformation from the shape variation due to articulated body motion, and characterizes segment surface deformation using PCA. An initial implementation of the method and the results demonstrated its effectiveness. In order to build a robust pose model, sufficient pose data is required. However, the availability of pose data is very limited. Besides, it needs to be realized that in reality, it may not be practical to use one pose model to represent the surface deformation over a larger range of pose changes.
3. The scheme developed for dynamic modeling uses 2-D video imagery as the input and provides a dynamic model as the output. Dynamic modeling is treated as an iterative process that consists of multiple steps. The emphasis is placed on computational convergence,

efficiency, and robustness, the common problems for dynamic modeling. For the dynamic modeling, the template model is important. It has to be parameterized and able to handle shape variation and surface deformation. While the models of such kind have been investigated and developed [8, 14], they are not available for public use. Implementing their methods and developing a customized dynamic template model is still a great challenge.

4. Based on a dynamic model, human activity can be replicated or created using marker data or joint angles. One important application of human activity replication and animation is M&S (modeling and simulation) based training. The high bio-fidelity provided by dynamic human modeling will enhance the representation and display of bio-signatures that are unique and critical to a particular mission and can thus improve the trainee's cognitive performance in real-world missions.

This project attained its goal to develop concepts and methodologies for dynamic human shape modeling. While major objectives have been achieved, significant efforts are still needed to address remaining issues. In particular, human shape data in various poses need to be collected for pose modeling, and the methods and algorithms developed need to be implemented on the test data sets. The end goal of human shape modeling is to develop a software tool or system that can be used to extract a dynamic model from 2-D video imagery or 3-D sensor data. To achieve that goal, major efforts are needed on technology implementation, software development, and system integration.

7.0 REFERENCES

1. Zhiqing Cheng and Kathleen Robinette, Static and Dynamic Human Shape Modeling – A Review of the Literature and State of the Art, Technical report, Air Force Research Laboratory, AFRL-RH-WP-TR-2010-0023, 2010.
2. Dennis Burnsides, INTEGRATE 2.8: A New Generation Three-Dimensional Visualization, Analysis, and Manipulation Utility, Technical report, Air Force Research Laboratory, AFRL-HE-WP-TR-2004-0169, 2004.
3. Kathleen Robinette et al., Civilian American and European Surface Anthropometry Resource (CAESAR), Final report, Air Force Research Laboratory, 2002.
4. Allen, B., Curless, B., and Popvic, Z. (2003). "The space of human body shapes: reconstruction and parameterization from range scans," in ACM SIGGRAPH 2003, 27-31 July 2003, San Diego, CA, USA.
5. Ben Azouz, B.Z., Rioux, M., Shu, C., and Lepage, R. (2005a). "Characterizing Human Shape Variation Using 3-D Anthropometric Data," International Journal of Computer Graphics, volume 22, number 5, pp. 302-314, 2005.
6. Hohenstein, Uniform Body Representation, Workpackage Input, E-Tailor project, IST-1999-10549.
7. H.Seo, N. Magnenat-Thalmann, An example-based approach to human body manipulation, Graphical Models 66 (2004) 1-23.

8. Anguelov, D., Srinivasan, P., Koller, D., Thrun, S., Rodgers, J. and Davis, J. (2005b). "SCAPE: Shape Completion and Animation of People." ACM Transactions on Graphics (SIGGRAPH) 24(3).
9. Davis, J., Marschner, S., Garr, M., and Levoy, M. (2002). "Filling Holes in Complex Surfaces Using Volumetric Diffusion", in: Symposium on 3-D Data Processing, Visualization, and Transmission.
10. Chui, H. and Rangarajan, A. (2000). "A new point matching algorithm for non-rigid registration", in: Proceedings of the Conference on Computer Vision and Pattern Recognition (CVPR)
11. Rusinkiewicz, S. and Levoy, M. (2001). "Efficient variants of the ICP algorithm", in: Proc. 3DIM, Quebec City, Canada, 2001. IEEEComputer Society.
12. Anguelov, D., Koller, D., Pang, H.C., Srinivasan, P., and Thrun, S. (2004). "Recovering Articulated Object Models from 3D Range Data," in Proceedings of the 20th conference on Uncertainty in artificial intelligence, Pages: 18 – 26, 2004.
13. Anguelov, D., Srinivasan, P., Pang, H.C., Koller, D., Thrun, S., and Davis, J. (2005a). "The correlated correspondence algorithm for unsupervised registration of nonrigid surfaces," Advances in Neural Information Processing Systems 17, 33-40.
14. Hasler, N. Stoll, C., Sunkel, M., Rosenhahn, B., and Seidel H.-P., A Statistical Model of Human Pose and Body Shape, EuroGraphics, Vol 28 No. 2, 2009.
15. Balan, A., Sigal, L., Black, M., Davis, J., and Haussecker, H.: Detailed Human Shape and Pose from Images. In: IEEE Conf. on Comp. Vision and Pattern Recognition (CVPR) (2007).
16. C. Sminchisescu and A. Telea. Human pose estimation from silhouettes a consistent approach using distance level sets. *WSCG Int. Conf. Computer Graphics, Visualization and Computer Vision*, 2002.
17. C. Stauffer and W. Grimson, "Adaptive background mixture models for real-time tracking," *Proceedings of the IEEE Computer Society Conference on Computer Vision and Pattern Recognition*, Vol. 2, pp. 246-252, (1999)
18. Aguiar, E., Zayer, R., Theobalt, C., Magnor, M., Seidel, H.P.: A Framework for Natural Animation of Digitized Models. In MPI-I-2006-4-003 (2006).

8.0 GLOSSARY/ACRONYMS

2-D	Two-Dimensional
3-D	Three-Dimensional
CAESAR	Civilian American and European Surface Anthropometry Resource
CPU	Central Processing Unit
GPU	Graphics Processing Unit
GRBF	Gaussian Radial Basis Function
HSL	Human Signatures Laboratory
IPCA	Incremental Principal Component Analysis
ISA	Instruction Set Architecture
M&S	Modeling and Simulation
PCA	Principal Component Analysis
PC	Principal Component
SCAPE	Shape Completion and Animation of PEople